

https://doi.org/10.3799/dqkx.2021.062



闽西南 E-MORB 型基性岩墙成因:来自地球化学、锆石 U-Pb 年代学及 Sr-Nd 同位素证据

张贵山^{1,2}, 彭仁¹, 温汉捷^{1,3*}, 赵志琦¹, 张磊¹, 邱红信¹, 孟乾坤¹

1. 长安大学地球科学与资源学院, 陕西西安 710054
2. 国土资源部岩浆作用成矿与找矿重点实验室, 陕西西安 710054
3. 中国科学院地球化学研究所矿床地球化学国家重点实验室, 贵州贵阳 550081

摘要: 闽西南地区发育富集洋脊玄武岩(E-MORB)地球化学特征的基性岩墙,这对研究晚中生代中国东南部的构造岩浆作用具有重要指示意义.利用岩石学、锆石 U-Pb 年代学、元素地球化学、同位素地球化学等方法对早白垩世闽西南基性岩墙进行研究,岩墙以辉绿岩和角闪辉长辉绿岩为主,属于中-低钾岩石系列, $Mg^{\#}$ 值为 55.80~66.38. 锆石 U-Pb 年龄为 117.4 ± 3.8 Ma,为早白垩世晚期岩浆活动的产物.样品富集 Rb、Ba、U、K、LREE 等元素,无明显 Nb、Ta、Ti 亏损,显示出 E-MORB 的地球化学特征; $(^{87}\text{Sr}/^{86}\text{Sr})_i = 0.70650 \sim 0.71019$, $\epsilon_{\text{Nd}}(t) = -0.9 \sim 4.0$, 同位素 Sr 中等富集、Nd 弱亏损.成岩过程有少量橄榄石和单斜辉石的分离结晶作用,无明显地壳混染作用.由于太平洋板块受南岭 E-W 向巨厚岩石圈的阻碍,导致板片下插速率与邻区产生差异,局部撕裂形成板片窗,软流圈地幔物质沿“窗口”上涌并卷裹起板片上的海洋沉积物,在上升中发生交代作用形成具有 E-MORB 特征的地幔岩.在早白垩世晚期的大陆拉张-陆内初始裂谷背景下,伴随软流圈上涌富集地幔岩发生部分熔融,形成的基性岩浆上侵形成了闽西南基性岩墙.

关键词: 基性岩墙; E-MORB; 锆石 U-Pb 年代学; 地球化学; 闽西南.

中图分类号: P597; P581

文章编号: 1000-2383(2021)12-4230-17

收稿日期: 2021-02-11

Genesis of E-MORB-Like Mafic Dykes in Southwestern Fujian Province, SE China: Evidence from Geochemistry, Zircon U-Pb Geochronology and Sr-Nd Isotope

Zhang Guishan^{1,2}, Peng Ren¹, Wen Hanjie^{1,3*}, Zhao Zhiqi¹, Zhang Lei¹, Qiu Hongxin¹, Meng Qiankun¹

1. School of Earth Science and Resources, Chang'an University, Xi'an 710054, China
2. Key Laboratory for the Study of Focused Magmatism and Giant Ore Deposits, MLR, Xi'an 710054, China
3. State Key Laboratory of Ore Deposit Geochemistry, Institute of Geochemistry, Chinese Academy of Sciences, Guiyang 550081, China

Abstract: E-MORB-like mafic dykes are exposed in Southwest Fujian Province and record key information of tectonic-magmatism in Southeast China during Late Cenozoic. A comprehensive research of petrology, zircon U-Pb dating, elemental geochemistry and isotope geochemistry was carried out. Mafic dykes are composed of dolerite and hornblende gabbro dolerite, and possess middle-low potassic features, with the $Mg^{\#}$ values range from 55.80 to 66.38. Zircon U-Pb dating yield an age of 117.4 ± 3.8 Ma,

基金项目: 国家自然科学基金面上项目(No.41073027);中央高校基本业务费项目(Nos.2013G2271018,310827172003).

作者简介: 张贵山(1971-),男,教授,主要从事岩石地球化学研究. ORCID:0000-0002-4813-1128. E-mail:zygzh@chd.edu.cn

* **通讯作者:** 温汉捷, ORCID: 0000-0003-1961-4144. E-mail: wenhanjie@vip.gyig.ac.cn

引用格式: 张贵山, 彭仁, 温汉捷, 等, 2021. 闽西南 E-MORB 型基性岩墙成因:来自地球化学、锆石 U-Pb 年代学及 Sr-Nd 同位素证据. 地球科学, 46(12):4230-4246.

indicating that mafic dykes were emplaced at end of Early Cretaceous. Dykes enrich in Rb, Ba, U, K and LREE, without obvious depletion of Nb, Ta and Ti, which is consist with the E-MORB geochemical affinities. Samples have positive $\epsilon_{Nd}(t)$ (-0.9 to 4.0), and $(^{87}Sr/^{86}Sr)_i$ values range from 0.706 50 to 0.710 19. Geochemical compositions show that the olivine and clinopyroxene fractionation have occurred and crustal contamination did not played an important role during the emplacement. We propose a slab window model to interpret the formation of mafic dykes. Subduction speed of Pacific plate beneath Nanling area was decreased by the overlying thickened lithosphere, which lead to the subduction velocity of the plate to be different from that of the adjacent area, and resulted in the formation of slab windows. Asthenospheric material could rise through slab windows, and carried and interacted with oceanic sediments, forming the E-MORB-like mantle rocks. With the upwelling of asthenosphere, E-MORB-like mantle materials will undergo partially melt and the resulting melts will emplace to form mafic dykes with a continental extensional-intracontinental rift setting at end of Early Cretaceous.

Key words: mafic dyke; E-MORB; zircon U-Pb geochronology; geochemistry; Southwest Fujian.

0 引言

在伸展构造背景下由玄武质岩浆沿拉张裂隙快速上升侵位形成的基性岩墙,是判断伸展—拉张构造活动的标志和时间标尺,也是研究大陆伸展、裂解、地幔柱活动和古陆块拼合重建的关键证据之一(Hou *et al.*, 2008; Ernst, 2014; Peng, 2015). 在时空分布上,基性岩墙从太古代到新生代均有产出,且遍布全球各大陆,如南非的 Bushveld Complex 内发育的 2.70~2.66 Ga 基性岩墙群、印度 Deccan 大火成岩省内 65 Ma 基性岩墙群等(Ernst, 2014). 基性岩墙携带着大量地幔源区信息,其元素及同位素组成是探讨地幔属性、壳幔演化过程、地幔源区组分的重要记录,也是识别岩石圈动力学背景及演化历史的重要证据(李献华等, 1997; Zhao *et al.*, 2004; Zhang *et al.*, 2007, 2017; Ernst, 2014; Peng, 2015; Srivastava *et al.*, 2019; 张家辉等, 2020). 因此,基性岩墙在大陆动力学研究领域占据重要地位.

中国东南部晚中生代受古太平洋构造域控制,发生了大规模构造岩浆活动,形成了以长英质为主的巨型岩浆带. 在巨型岩浆带内基性岩、玄武岩出露规模虽小,但为研究中国东南部晚中生代的壳幔相互作用、地幔源区组成和岩浆岩成因等打开了“窗口”(Zhou *et al.*, 2006). 特别是中国东南部普遍发育白垩纪基性岩墙,从沿海到内陆均有出露. 基性岩墙是具有构造岩浆活动标志特征的岩石类型,对研究中国东南部晚中生代的伸展构造作用、岩石圈拉张期次、岩浆岩成因和大陆动力学背景演化等具有深远的意义,已成为研究中国东南部晚中生代岩浆作用重要对象(李献华等, 1997; Zhao *et al.*, 2004; Xie *et al.*, 2006; 张贵山等, 2007; Zhang *et al.*, 2007; 曹建劲等, 2009; 董传万等, 2010; 陈新跃等, 2014; 丁聪等, 2015; 雷祝梁等, 2019).

有关中国东南部晚中生代的构造岩浆活动重大基础科学问题,一直是国内外地质工作者关注的热点(John *et al.*, 1990; Gilder *et al.*, 1996; Lapierre *et al.* 1997; Zhou *et al.*, 2006; Li and Li, 2007; Liu *et al.*, 2016). 前人主要对长英质岩石进行岩石学、地球化学、同位素地质学等系统研究,积累了大量资料. 晚中生代构造岩浆活动机制有与古太平洋板块俯冲密切相关的观点(Lapierre *et al.*, 1997; Zhou *et al.*, 2006; Li and Li, 2007; Liu *et al.*, 2016); 也有未受到古太平洋俯冲系统影响的认识(Meng *et al.*, 2012). 关于构造—岩浆活动机制认识上存在差异的原因,是选择研究对象不同造成的. 事实上,中国东南部晚中生代除了大规模发育与洋壳俯冲作用相关的钙碱性、高钾钙碱性系列岩浆岩外,还出露与俯冲作用关系不密切,无 Nb、Ta 负异常、Sr-Nd 同位素弱亏损、具有 E-MORB 地球化学特征的岩石,这两类岩石在地球化学组成上差异明显. 中国东南部晚中生代处于统一大陆动力学控制下,发育两种截然不同地球化学组成特征的岩石,两者成因机制与大陆动力学控制机理等还需进一步深入研究.

南岭东段及闽西南地区发育具有 E-MORB 地球化学组成特征的基性岩墙,与具有俯冲交代成因特征的基性岩墙相比较, E-MORB 型基性岩墙分布地区局限,研究程度低,对其成因机制、地幔源区组成特征、古太平洋板块俯冲的影响程度、深部动力学机制等认识还不清晰.

因此,本文选择出露于闽西南 E-MORB 型基性岩墙作为研究对象,针对其岩浆起源与演化、源区组成特征、大地构造背景等做深入研究,进一步探讨中国东南部晚中生代构造—岩浆作用机制,为古太平洋俯冲作用对该地区岩浆活动、大地构造演化的响应提供限定.

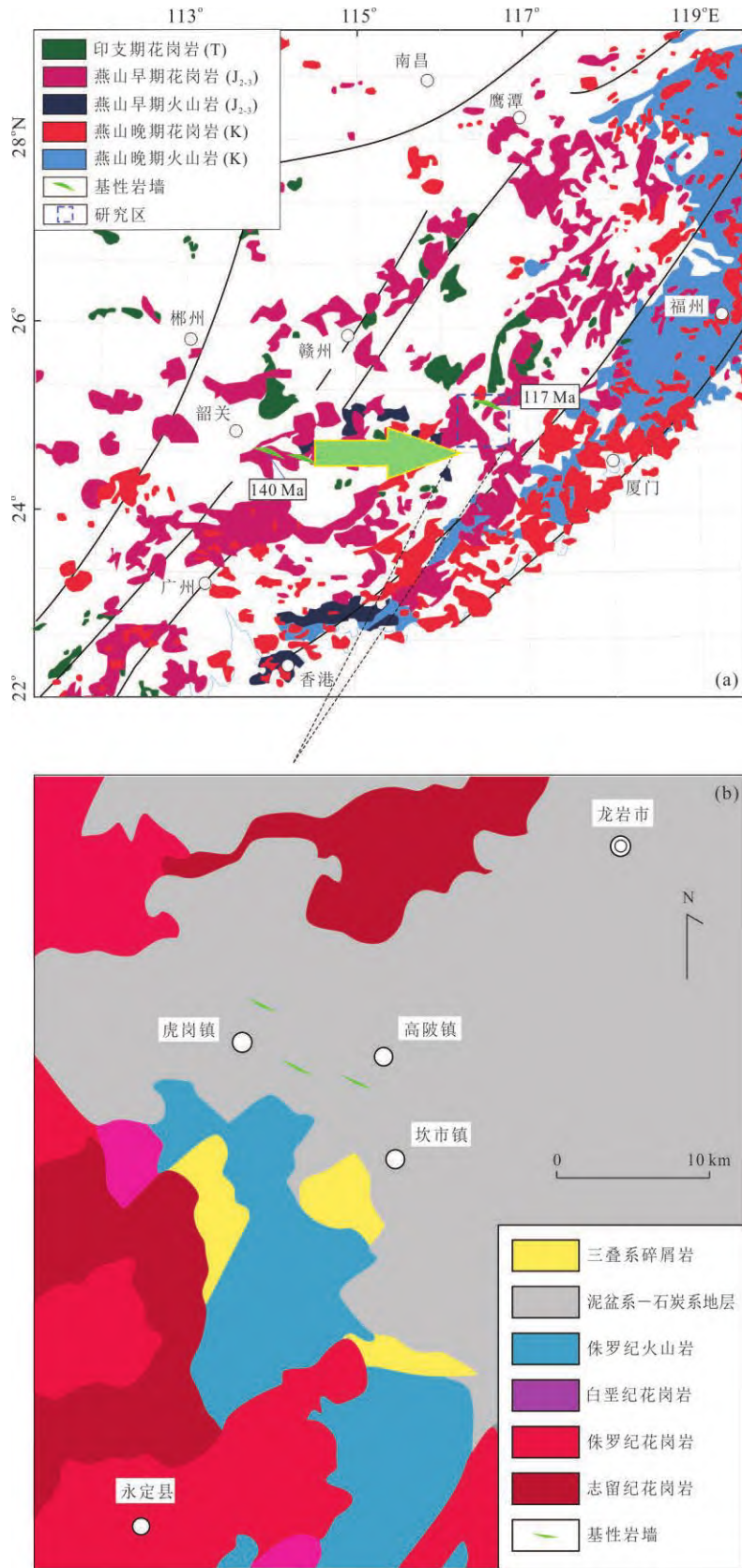


图 1 中国东南部中生代岩浆岩分布简图(a)和工作区地质简图(b)

Fig.1 Distribution of Mesozoic granite-volcanic rocks in Southeast China (a) and overview map showing the distribution of mafic dykes in the Southwest Fujian (b)

a 据 Zhou *et al.* (2006) 修改; b 据 黄泉祯等 (1998) 修改

1 地质背景与样品

中国东南部位于欧亚大陆边缘南段,是环太平洋构造—岩浆带的重要组成部分(Zhou *et al.*, 2006). 区域地壳由中元古代基底、古生代海相沉积盖层和中生代陆相火山沉积岩构成,并被大量花岗质岩石侵入. 从太古代起至少经历过5期重要的构造—岩浆事件,对中国东南部大陆的形成、大地构造演化、岩浆活动产生了深远影响. 印支期造山旋回造就了大规模的构造变形和S型花岗质岩浆活动,燕山期受古太平洋板块俯冲的影响,诱发了大规模岩浆活动和成矿作用(Liu *et al.*, 2016). 晚中生代中国东南部岩浆活动严格受NE向构造体系控制,赣江断裂带是中生代火山岩的边界线,政和—大浦断裂带是S、I型花岗岩的分界线,长乐—南澳断裂带控制着早白垩世晚期变形和晚白垩世岩浆岩的分布(Shu *et al.*, 2009). 在构造—岩浆活动综合作用下,中国东南部形成了独特的巨型晚中生代岩浆岩带(图1a).

研究区位于福建永定盆地北部(图1b),区内发育寒武系碎屑沉积岩地层,晚古生代海—陆相地层,三叠系陆相含煤沉积地层,侏罗系基性、酸性火山岩系与碎屑沉积地层;侵入岩体为志留纪的钾长花岗岩与二长花岗岩,早—晚侏罗世钾长花岗岩,早白垩世的黑云母二长花岗岩与花岗闪长岩(图1b). 火山岩为早—中侏罗世双峰式火山岩.

基性岩墙出露于永定火山岩盆地北部(图1b),侵位在晚古生代地层中,呈NW向展布,倾角 $75^{\circ}\sim 85^{\circ}$,岩墙长约数百米. 虎岗镇(HG)和黄泥塘(HNT)为灰绿色辉绿岩(图2),辉绿结构和致密块状构造,矿物组成为斜长石、辉石、绿泥石和钛磁铁矿等;斜长石为板状、长片状、长条状,自形晶;辉石为普通辉石,短柱状和粒状,半自形—他形晶;绿泥石为片状,他形. 西陂(XP)为灰绿色角闪辉长辉绿岩,辉长辉绿结构和致密块状构造. 矿物组成为斜长石、角闪石、辉石、磁铁矿和磷灰石等;斜长石呈板状和长片状,自形晶;辉石为他形,部分辉石见有纤闪石化蚀变;角闪石为长柱状,多色性发育.



图2 闽西南基性岩墙标本与镜下正交偏光照片

Fig.2 Orthogonal polarized photographs of the mafic dykes in Southwest Fujian

Pl.斜长石, Cpx.单斜辉石, Chl.绿泥石, Ilm. 钛铁矿

2 分析测试方法

主量元素在长安大学西部矿产资源与地质工程教育部重点实验室完成,采用 LAB CENTER XRF-1800 型 X 射线荧光光谱仪分析,精度优于 5%。微量元素分析在中国科学院地球化学研究所矿床地球化学国家重点实验室完成;所用仪器为 ELAN-DRC-e ICP-MS,分析精度优于 5%,分析测试方法见 Qi *et al.* (2000)。

全岩 Sr-Nd 同位素组成用 Neptune MC-ICP-MS 分析,在中国科学院广州地球化学研究所同位素地球化学国家重点实验室完成。简要分析流程:全岩粉末在 Teflon 杯中,用 HNO₃ 和 HF 混合酸消解,经专用的阳离子交换柱分离后上机测试,详细流程见梁细荣等 (2003)。样品的 ⁸⁷Sr/⁸⁶Sr 和 ¹⁴³Nd/¹⁴⁴Nd 比值分别用 ⁸⁶Sr/⁸⁸Sr=0.119 4 和 ¹⁴⁶Nd/¹⁴⁴Nd=0.721 9 标准化,并用国际标样 NBS987 (⁸⁷Sr/⁸⁶Sr=0.710 248) 和 Shin Etsu JNdi-1 (¹⁴³Nd/¹⁴⁴Nd=0.512 115) 进行校正。

锆石阴极发光照相 (CL) 和 U-Pb 年代学测试在西北大学大陆动力学国家重点实验室完成。锆石激光剥蚀—等离子质谱采用 Hewlett Packard 公司生产的 Agilent7500a ICP-MS 测定,激光剥蚀系统为 GeoLas 200M 型激光剥蚀系统,激光器为 193 nm ARF 准分子激光器,束斑直径为 25 μm。锆石 U-Pb 年龄以国际标准锆石 91500 为外标进行校正,每隔 5 个测点测定一次标样;元素含量以 NIST610 为外

标,²⁹Si 为内标,每隔 10 个测点测定一次标样,保证标样和样品的仪器测试条件完全一致,详细流程见文献 Yuan *et al.* (2008)。数据处理采用 Glitter4.0 软件,并按照 Andersen (2002) 的方法进行普通铅校正,年龄计算及相关谐和图制作等用 Isoplot3.75 软件完成。

3 结果

3.1 锆石 U-Pb 年代学

基性岩墙样品 (约 20 kg) 分选的锆石 (约 80 粒),多为灰白色、淡棕色,颗粒大小不等,自形程度完好,多为柱状、四方双锥状,粒径 50~130 μm,长宽比 1.5:1.0~4.0:1.0。锆石的阴极发光 (CL) 图像及分析点位见图 3,锆石发育典型岩浆振荡环带 (图 3)。

闽西南基性岩墙锆石中 Th 含量为 892.0~60.5 μg/g、U 含量为 1 335.0~85.6 μg/g, Th/U=0.35~1.61。投到锆石 U-Pb 谐和图上分成两个群组,其中一个群组有 15 个测点聚集,加权平均 ²⁰⁶Pb/²³⁸U 年龄为 117.4±3.8 Ma (MSWD=2.3) (图 4b);另一个测试点的年龄为 421 Ma (附表 1 和图 4a),为继承锆石年龄,与闽西和赣南地区发育的志留纪花岗岩年代相近 (崔圆圆等, 2013)。

3.2 主量元素

全岩地球化学分析数据见附表 2。SiO₂=47.74%~49.47%、K₂O=0.16%~0.85%、Na₂O=1.36%~2.37%; Na₂O/K₂O=2.13~14.81, 平均值

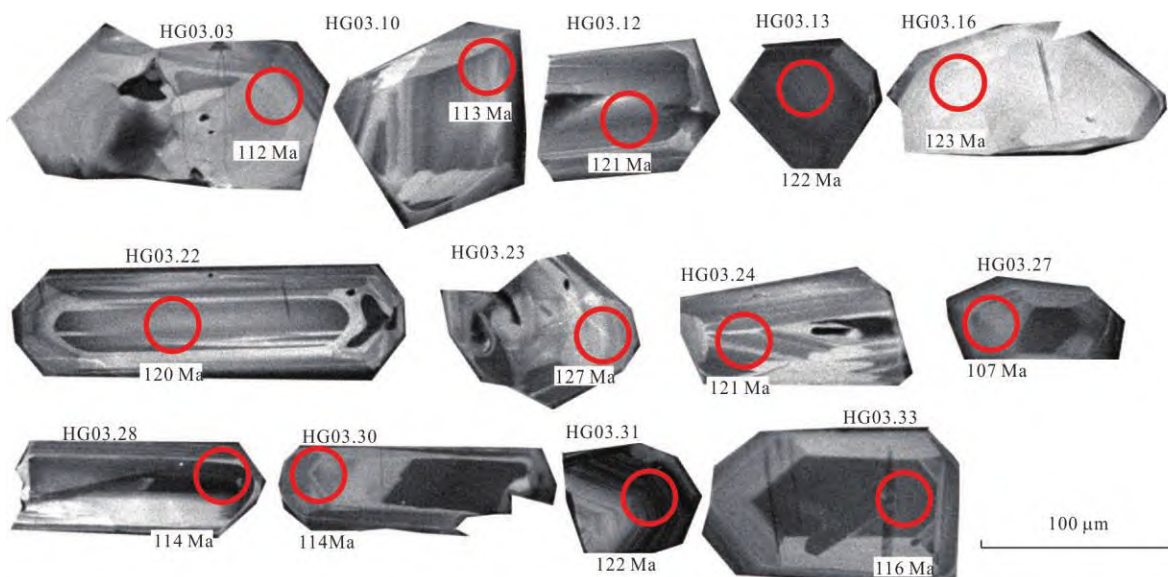


图 3 闽西南基性岩墙锆石颗粒部分 CL 图像及 LA-ICP-MS 分析点

Fig.3 Representative cathodoluminescence (CL) images for zircons from dykes

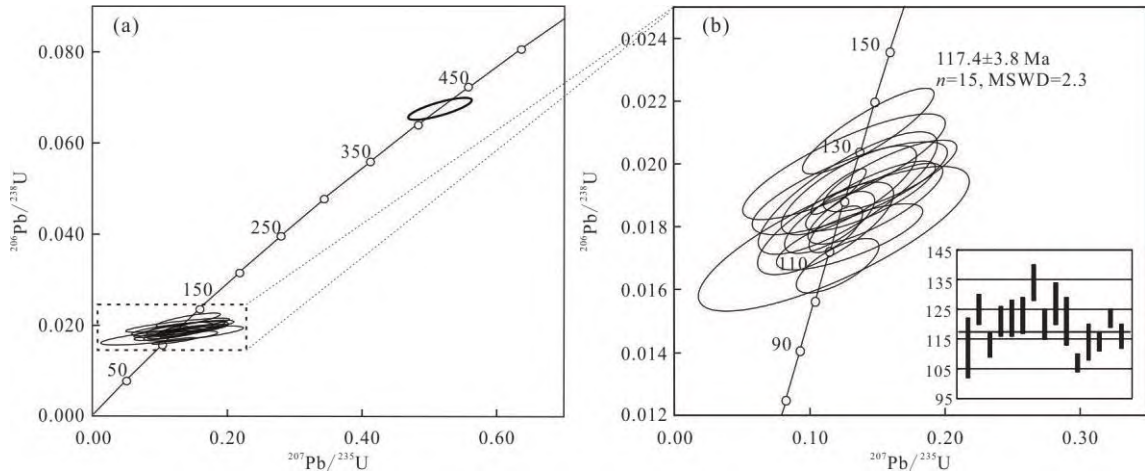


图 4 闽西南基性岩墙锆石 U-Pb 年龄图解

Fig.4 Zircon U-Pb concordia plots and calculated $^{206}\text{Pb}/^{238}\text{U}$ ages of mafic dykes in the Southwest Fujian

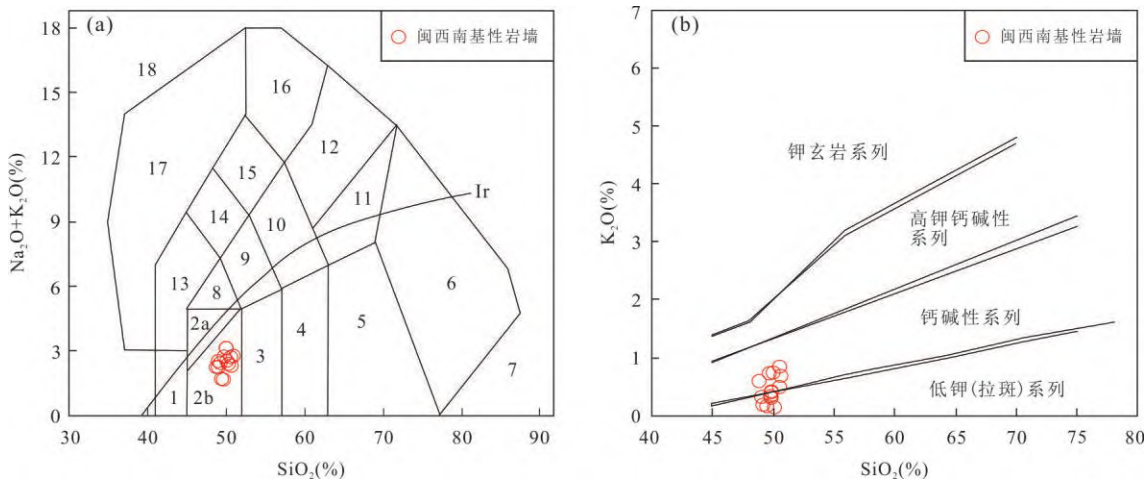


图 5 闽西南基性岩墙 TAS(a)与 $\text{SiO}_2\text{-K}_2\text{O}$ (b)图解

Fig.5 $\text{K}_2\text{O}+\text{Na}_2\text{O}$ vs. SiO_2 diagram (a), K_2O vs. SiO_2 diagram (b) for mafic dykes from Southwest Fujian

图 a 引自 Middlemost(1994); 图 b 底图引自 Rickwood(1989); a-Irvine 分界线, 上方为碱性, 下方为亚碱性; 1. 橄辉岩; 2a. 碱性辉岩; 2b. 亚碱性辉岩; 3. 辉长闪岩; 4. 闪岩; 5. 花岗闪岩; 6. 花岗岩; 7. 石英岩; 8. 二长辉岩; 9. 二长闪岩; 10. 二长岩; 11. 石英二长岩; 12. 正长岩; 13. 副长石辉岩; 14. 副长石二长闪岩; 15. 副长石二长正长岩; 16. 副长正长岩; 17. 副长深成岩; 18. 霓方钠岩/磷霞岩/粗白榴岩

为 6.46; $\text{Mg}^\#$ 值介于 55.80~66.38, 平均值为 61.96. 在图 5 中, 分别落在亚碱性系列 (图 5a) 和中-低钾系列范畴内 (图 5b). 在图 6 中, MgO 与 TiO_2 、 $\text{K}_2\text{O}+\text{Na}_2\text{O}$ 、 TFeO 和 Fe_2O_3 负相关, 且与 Ni 、 Cr 正相关.

3.3 稀土和微量元素

稀土和微量元素分析结果见附表 2, 基性岩墙稀土总量 ($\sum\text{REE}$) 为 47.3~66.1 $\mu\text{g/g}$ 、轻重稀土比值 ($\sum\text{LREE}/\sum\text{HREE}$) 在 2.55~3.73 之间变化、 $(\text{La}/\text{Yb})_n$ 的变化范围为 1.85~3.13. 球粒陨石标准化配分曲线为右倾弱富集型 (图 7a), 与富集洋中脊玄武岩 (E-MORB) 稀土元素配分特征相似, 与洋岛玄武岩

(OIB)、大洋中脊玄武岩 (N-MORB)、中国东南部的中侏罗世和新生代玄武岩的稀土元素配分特征差异较大. 无明显 δEu 和 δCe 异常, $\delta\text{Eu}=0.95\sim1.22$ (平均值 1.09), $\delta\text{Ce}=0.94\sim1.02$ (平均值 0.98).

不相容元素 N-MORB 标准化“蛛网图”(图 7b) 中, Rb 、 Ba 、 U 和 K 呈富集趋势, 无显著 Nb 、 Ta 、 Ti 负异常, 与 E-MORB 特征相似, 与 OIB、中国东南部的中侏罗世和新生代玄武岩的差异明显. 相容元素 Ni 含量 62.0~147.0 $\mu\text{g/g}$ (平均值为 95.8 $\mu\text{g/g}$), Cr 含量为 150~388 $\mu\text{g/g}$ (平均值为 248 $\mu\text{g/g}$).

3.4 Sr-Nd 同位素特征

Sr-Nd 同位素组成见附表 3. 虎岗镇样品

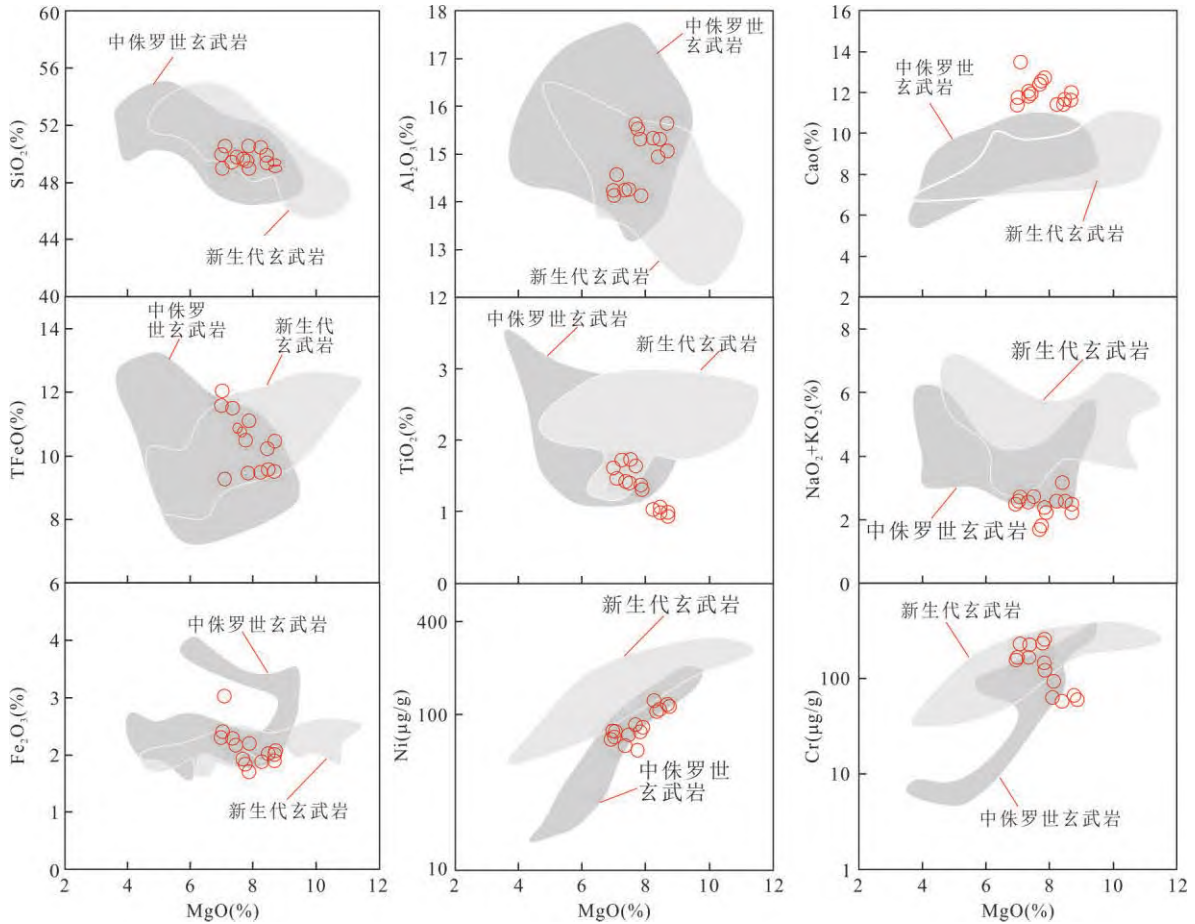


图 6 闽西南基性岩墙 MgO 横坐标 Hark 图解

Fig.6 Hark diagrams for the mafic dykes from Southwest Fujian

新生代玄武岩数据引自 Zou *et al.*(2000); Ho *et al.*(2003); Li *et al.*(2015); 杨金豹 (2015). 中侏罗世玄武岩引自孔兴功(2001); Li *et al.*(2003); Wang *et al.*(2005)

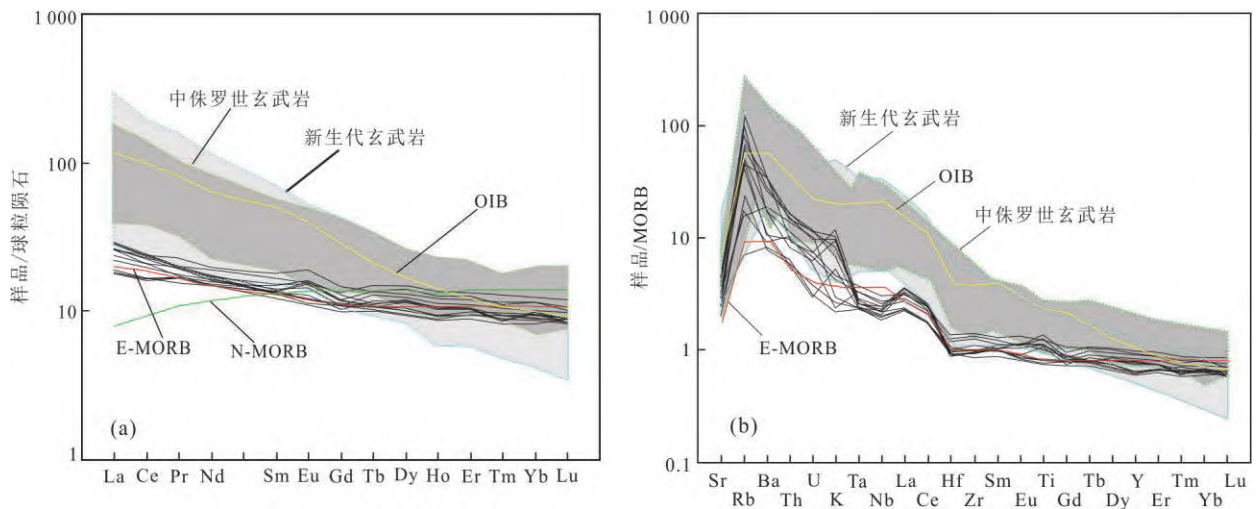


图 7 闽西南基性岩墙稀土元素配分模式图(a)与微量元素蛛网图(b)

Fig.7 Chondrite-normalized rare earth element patterns (a) and MORB-normalized trace element diagram (b) for the mafic dykes from Southwest Fujian

球粒陨石与 MORB 标准化数据、OIB、N-MORB、E-MORB 均引自 Sun and McDonough(1989); 新生代玄武岩数据引自 Zou *et al.*(2000); Ho *et al.*(2003); Li *et al.*(2015); 杨金豹 (2015); 中侏罗世玄武岩引自孔兴功(2001); Li *et al.*(2003); Wang *et al.*(2005)

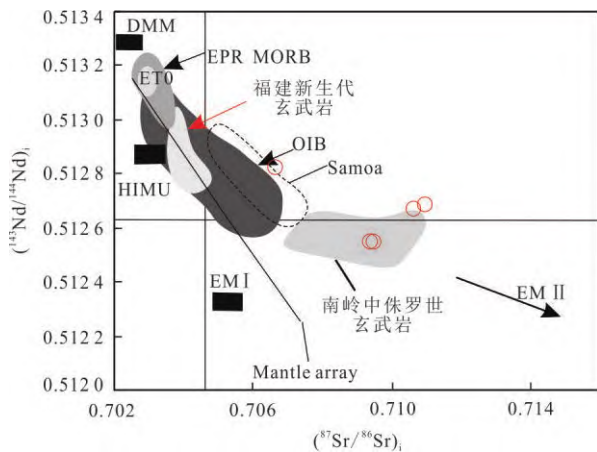


图 8 闽西南基性岩墙 Sr—Nd 同位素图

Fig.8 $(^{87}\text{Sr}/^{86}\text{Sr})_i$ vs. $(^{143}\text{Nd}/^{144}\text{Nd})_i$ for the mafic dykes from Southwest Fujian

EM I, EM II, DMM, HIMU 引自 Zindler and Hart (1986); 福建新生代玄武岩引自 Zou *et al.* (2000); Ho *et al.* (2003); 南岭中侏罗世玄武岩引自 孔兴功 (2001); Li *et al.* (2003); Wang *et al.* (2005); Zhou *et al.* (2006)

$(^{87}\text{Sr}/^{86}\text{Sr})_i$ 值为 0.710 18 和 0.710 19、 $\epsilon_{\text{Nd}}(t)$ 值为 1.4 和 1.6, 显示弱亏损的同位素组成特征; 黄泥塘样品 $(^{87}\text{Sr}/^{86}\text{Sr})_i = 0.706 50$ 、 $\epsilon_{\text{Nd}}(t) = 4.0$, 明显亏损特征; 西陂 $(^{87}\text{Sr}/^{86}\text{Sr})_i$ 值为 0.708 39 和 0.709 00 及 $\epsilon_{\text{Nd}}(t)$ 值为 -0.7 和 -0.9. 在 Sr-Nd 同位素图解 (图 8) 中, 虎岗镇和西陂样品投在南岭中侏罗世火山岩范畴内, 黄泥塘样品稍亏损.

4 讨论

4.1 基性岩墙形成时代

大量研究工作表明, 中国东南部晚中生代存在多期伸展构造活动, 同期次的基性岩墙 (岩脉) 普遍产出 (李献华等, 1997; Xie *et al.*, 2006; 张贵山等, 2007; Zhao *et al.*, 2007; 曹建劲等, 2009; 董传万等, 2010; 唐立梅等, 2010; 丁聪等, 2015), 早期研究多采用全岩 K-Ar 法确定其侵位时代 (如李献华等, 1997; Xie *et al.*, 2006), 随着锆石 U-Pb、全岩 ^{39}Ar - ^{40}Ar 等方法的应用, 基性岩墙的高精度年代学数据不断积累 (董传万等, 2010, 2011; 秦社彩等, 2010; 唐立梅等, 2010; 丁聪等, 2015; Wang *et al.*, 2018; Yang *et al.*, 2018), 促进了基性岩墙侵位与区域伸展拉张期次关系的研究. 本文锆石岩浆震荡环带发育 (图 3)、Th/U 比值 (0.35~1.61), 符合岩浆锆石特征, 为岩浆结晶锆石. 同位素年龄数据谐和度高, 说明锆石 U-Pb 体系保持封闭. 因此, 锆石 U-Pb

年龄 (117.4 ± 3.8 Ma) 代表了基性岩墙的侵位时间.

基性岩墙是岩石圈伸展拉张构造体制下岩浆侵位的产物, 侵位年龄代表了伸展构造活动期次. 闽西南基性岩墙的产出, 指示了区域上存在一期伸展构造活动. 根据锆石 U-Pb 高精度同位素测年数据 (117.4 ± 3.8 Ma), 综合区域上平潭、泉州辉长岩体锆石 U-Pb 年龄分别为 115 Ma 和 113 Ma (Zhang *et al.*, 2019)、江西基性岩墙全岩 K-Ar (118.5 Ma) (Xie *et al.*, 2006) 等年龄数据, 认为中国东南部早白垩世晚期 (~115 Ma) 有一期伸展构造活动.

4.2 地壳混染与分离结晶作用

岩浆侵位前熔体可能经历了一系列演化过程, 如地壳物质混染和结晶分异, 可能改变原始岩浆的组成. 因此, 讨论岩浆源区的特征之前, 需要评价结晶分异与地壳混染作用对原始岩浆的影响.

元素对比值可以指示岩浆演化过程, 如: Nb/La 比值是鉴别地壳混染作用的有效指标. 原始地幔和 MORB 的 Nb/La 比值都接近于 1.0 (Hofmann, 1988), 大陆地壳的比值约为 0.63 (Wedepohl, 1995), 若基性岩浆发生地壳混染作用, Nb/La 比值应落在地幔与大陆地壳之间. 闽西南基性岩墙 (虎岗) 的 Nb/La 比值 (0.58~0.66, 均值为 0.61) 接近地壳值, 落在大陆地壳端元附近, 说明虎岗基性岩墙的 Nb/La 比值不可能是大陆地壳混染作用造成的; 黄泥塘 (HNT) 和西陂 (XP) Nb/La 比值 (0.76~0.89, 均值 0.82) 落在原始地幔与地壳之间, 表明有地壳物质的参与, 但两者的 $^{87}\text{Sr}/^{86}\text{Sr}$ 与 $\text{SiO}_2/^{86}\text{Sr}$ 之间没有显著相关性, 说明地壳物质是在源区加入的, 不是陆壳物质混染作用的结果. 选用 La/Yb、Ce/Yb、Nb/Yb、Th/Yb 等元素对比值进行判别 (图 9), 闽西南基性岩墙分散于原始地幔和 MORB 附近, 没有大陆地壳物质混染作用特征的显示. 因此, 闽西南基性岩墙应源于幔源基性岩浆, 后期没有受到明显陆壳物质混染的影响.

闽西南基性岩墙 MgO 含量在 6.89%~8.55%, $\text{Mg}^\#$ 介于 55.80~66.38, 表明岩浆结晶分异程度较弱. MgO 与 Ni、CaO 正相关, 与 TiO_2 、TFeO 和 Fe_2O_3 负相关 (图 6), 岩浆经历一定的橄榄石、单斜辉石、铁钛氧化物的分离结晶作用.

4.3 地幔源区特征

闽西南基性岩墙的微量元素蛛网图及稀土元素配分图与富集型洋中脊玄武岩 (E-MORB) 的相似, 不同于大洋中脊玄武岩 (N-MORB)、洋岛玄武

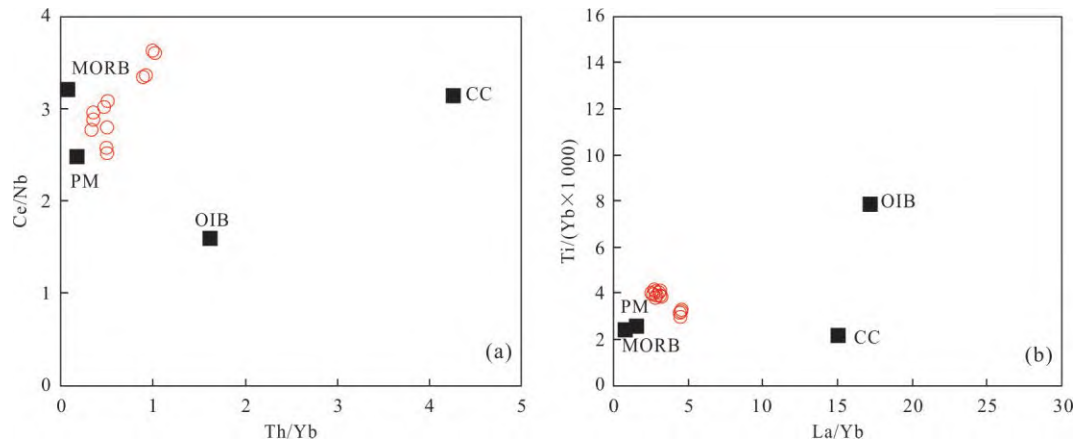


图9 闽西南基性岩墙 Th/Yb—Ce/Nb和 La/Yb—Ti/(Yb×1 000)判别图

Fig.9 Th/Yb vs.Ce/Nb and La/Yb vs.Ti/(Yb×1 000) discriminant diagrams of the mafic dykes from Southwest Fujian PM(原始地幔)、MORB(洋中脊玄武岩)、OIB(洋岛玄武岩)引自 Sun and McDonough(1989);CC(大陆地壳)引自 Wedepohl(1995)

岩(OIB)、中国东南部的中侏罗世与新生代玄武岩。由图10可知,闽西南及南岭地区部分基性岩墙样品点分布于E-MORB范畴内,部分样品落在E-MORB上部;中国东南部新生代玄武岩投到OIB范畴。根据不同学者给出的E-MORB划分标准($K_2O/TiO_2 > 0.11$ 、 $(La/Sm)_N \geq 1$ 、 $Sr > 180 \mu g/g$ 、 $\Delta Nb = 1.74 + \lg(Nb/Y) - 1.92 \lg(Zr/Y) > 0$) (Fitton *et al.*, 1997; Smith *et al.*, 2001; Hall *et al.*, 2006; Arevalo *et al.*, 2009),闽西南基性岩墙的 K_2O/TiO_2 (0.11~0.76)、 $(La/Sm)_N$ (1.23~2.18)、 Sr (183~419 $\mu g/g$)、 ΔNb (-0.022~0.093,平均值为0.058)值均落在E-MORB划分范畴内,具有E-MORB地球化学特征。因此,闽西南基性岩墙的源区、成岩过程可能与E-MORB相类似。

与形成于大洋板内或大洋弧后盆地的E-MORB相比,闽西南基性岩墙形成于陆内环境,两者形成的大地构造背景迥异,却有相似的地球化学特征,推测两者源区有相似的形成机制。富集型洋脊玄武岩(E-MORB)成因模型有亏损地幔(DM)与富集地幔(EM)混合(Niu *et al.*, 2002; Donnelly *et al.*, 2004)、起源于地幔交代作用形成的富集地幔(Donnelly *et al.*, 2004)、俯冲大洋地壳再循环形成的石榴石辉石岩或榴辉岩(Hirschmann and Stolper, 1996)、厚重板块快速俯冲发生板片断裂和拆离形成一个裂隙,下部富集地幔减压上涌部分熔融而形成(Dilek, 2006)等。晚中生代古太平洋板块持续俯冲作用,改造了中国东南部岩石圈地幔,形成了巨型大地幔楔,由上覆地幔楔部分熔融形成的玄武质岩浆具有亏损Nb、Ta、Ti的地球化学特征(Zhou

et al., 2006),显然地幔楔不是闽西南基性岩墙的源区。闽西南基性岩墙的Zr/Nb比值落在东太平洋富集洋脊玄武岩(EPR、E-MORB)范畴内(表1),表1显示其他元素对比值均高于东太平洋的富集洋脊玄武岩(Shimizu *et al.*, 2016),表明其源区比EPR(E-MORB)还要富集。表1显示基性岩墙的La/Nb、K/Nb、Th/Nb比值明显低于大洋沉积物,其他元素接近大洋沉积物的比值范围(Plank and Ludden, 1992),说明基性岩墙的源区有大洋沉积物的参与。闽西南基性岩墙弱亏损的Sr-Nd同位素特征($\epsilon_{Nd}(t) = -0.9 \sim 4.0$),反映出其源区存在大洋沉积物参与作用。

中生代以来,太平洋板块持续向NW俯冲于中国东南部大陆板块之下,俯冲板片将大洋沉积物带入地幔内,在地幔中其发生了低度部分熔融作用,产生的熔体与地幔橄榄岩发生地幔交代作用,形成具有E-MORB地球化学特征的富集地幔岩(Niu *et al.*, 2002),伴随着软流圈地幔强烈上涌将富集地幔岩携带上升到浅部,绝热减压发生部分熔融,形成了具有E-MORB特征的闽西南基性岩墙原始岩浆。

4.4 构造意义

闽西南地区是南岭东段一部分,与赣南和粤东北处于同一大地构造背景范畴。闽西南基性岩墙样品的Zr/Y比值在3.23~4.01之间变化,指示了板内构造环境特征。在Zr/Y—Zr图解中,样品处于洋中脊玄武岩和板内玄武岩范围。图11a中,样品投入到大陆拉斑玄武岩及靠近富集型洋脊玄武岩区域。图11b中,投入到钙碱性玄武岩、富集洋中脊玄武岩+

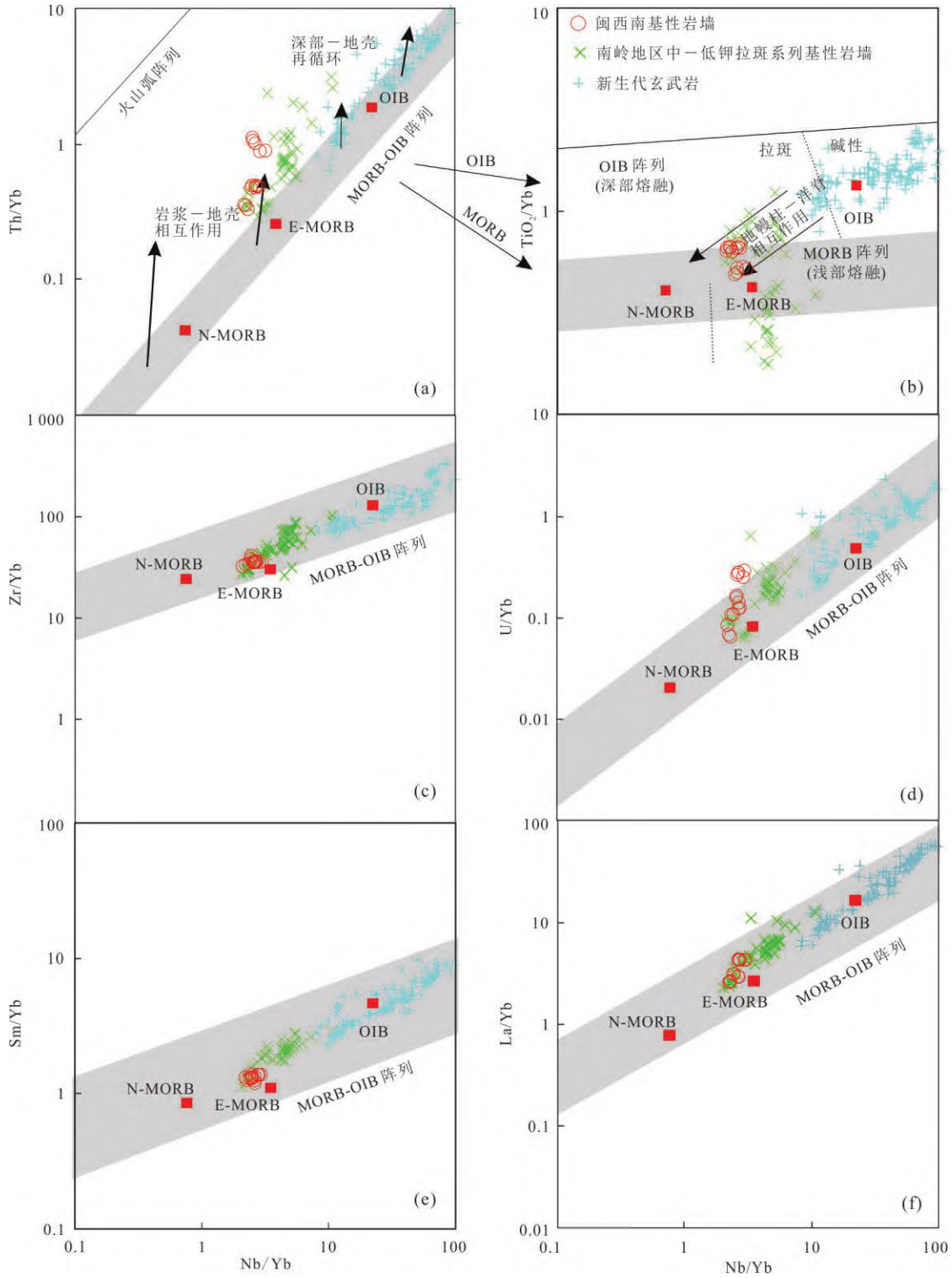


图 10 闽西南基性岩墙以 Nb/Yb 为横坐标的相关判别图解

Fig.10 Nb/Yb discriminant diagrams for mafic dykes from Southwest Fujian
图 a、b 底图引自 Pearce(2008); 图 c~h 底图引自 Green(2006); Maurice *et al.*(2012)

板内拉斑玄武岩区域,显示从钙碱性玄武岩向富集洋脊玄武岩+板内拉斑玄武岩变化的趋势.图 11c 中,投入大陆拉张带玄武岩区、陆内初始裂谷及陆缘裂谷拉斑玄武岩区内.综合南岭东段的富集大洋

中脊玄武岩特征、 $\epsilon_{Nd}(t) > 0$ 、较高 Sr 同位素初始值的基性岩墙(李献华等,1997; Xie *et al.*, 2006; 曹建劲等, 2009), 将其投入上述相关图解, 与闽西南同样投入相同区域. 因此, 结合闽西南及南岭东段基

表 1 闽西南晚中生代基性岩墙与各端元微量元素浓度比值对比

Table 1 Comparison of trace element ratios for different end-members and the Late Mesozoic mafic dykes from the Southwest Fujian

	CC	PM	N-MORB	OIB	大洋沉积物	EPR(E-MORB)	本文
Zr/Nb	10.7	15.7	31.8	5.8	7.07~40.5 (11.5)	1.99~21.6 (5.70)	12.3~16.8 (14.5)
La/Nb	1.58	0.96	1.07	0.77	1.81~4.32 (2.63)	0.49~0.95 (0.61)	1.12~1.71 (1.36)
Ba/Nb	30.8	9.8	2.7	7.29	10.8~511 (68.2)	4.77~8.57 (6.01)	9.8~41.5 (22.5)
Rb/Nb	4.12	0.89	0.24	0.65	4.43~10.5 (7.05)	0.39~0.81 (0.53)	0.87~12.1 (5.31)
K/Nb	1 870	351	258	250	1 308~2 866 (1 726)	129~422 (210)	230~1 278 (672)
Th/Nb	0.45	0.12	0.052	0.083	0.21~1.44 (0.67)	0.058~0.085 (0.072)	0.15~0.39 (0.24)
Th/La	0.28	0.12	0.048	0.11	0.15~0.53 (0.26)	0.069~0.149 (0.12)	0.12~0.23 (0.17)
Ba/La	19.5	10.2	2.52	9.46	10.6~141 (25.8)	5.81~12.5 (9.96)	7.44~31.5 (15.9)
Ba/Th	68.7	82.2	52.5	87.5	14.8~554 (100)	65.9~131 (83.6)	47.6~198 (90.9)

注:CC(大陆地壳)引自 Wedepohl(1995);PM、N-MORB、OIB引自 Sun and McDonough(1989);大洋沉积物引自 Plank and Ludden(1992);EPR(东太平洋中脊)引自 Shimizu *et al.*(2016);括号内为平均值。

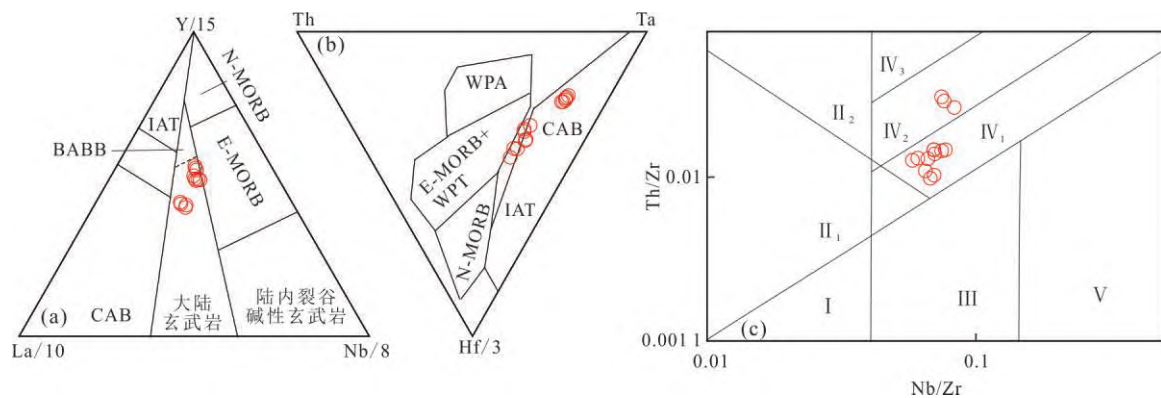


图 11 闽西南基性岩墙 Y/15-La/10-Nb/8(a)、Hf/3-Th-Ta(b)、Th/Zr-Nb/Zr(c)构造判别图解

Fig.11 Y/15-La/10-Nb/8 (a) and Hf/3-Th-Ta (b) and Nb/Zr-Th/Zr (c) tectonic setting discriminant diagrams for mafic dykes from Southwest Fujian

N-MORB.N型大洋中脊玄武岩;E-MORB.E型大洋中脊玄武岩;WPA.板内碱性玄武岩;CAB.钙碱性玄武岩;IAB.岛弧拉斑玄武岩;BABB.弧后盆地玄武岩;WPB.板内玄武岩;I.N-MORB.Ⅱ₁.陆缘岛弧火山岩;Ⅱ₂.陆缘火山玄武岩;Ⅲ.大洋板内玄武岩海山玄武岩;Ⅳ₁.陆内初始、陆缘裂谷拉斑玄武岩;Ⅳ₂.大陆拉张玄武岩;Ⅳ₃.大陆碰撞玄武岩区;V.地幔热柱玄武岩;图a底图引自 Cabanis and Lecolle (1989);图b底图引自 Wood(1980);图c底图引自孙书勤等(2003)

性岩墙的地球化学特征,初步判别其形成于大陆拉张带向陆内初始裂谷演化的构造体系。

闽西南基性岩墙无Nb、Ta、Ti负异常,Sr-Nd同位素组成呈现弱亏损,与洋壳俯冲交代作用形成的岩浆岩形成鲜明对比,表明闽西南基性岩墙的形成与太平洋板块俯冲交代的上覆地幔楔源区没有直接关系.闽西南是南岭构造带的一部分,南岭构造带形成于印支期古特提斯洋闭合及板块碰撞造山过程,主构造线呈近E-W向,指示其挤压变形的应力方向为近S-N向(徐先兵等,2009).南岭褶皱隆起造山导致地壳增厚和岩石圈加厚(Sun *et al.*, 2005; Song *et al.*, 2017),E-W向巨厚岩石圈横亘于华南,巨厚岩石圈可能阻碍了晚中生代古太平洋板块的

NW向快速俯冲,导致下插到南岭地区的板片俯冲相对速率下降,与福建北部、浙江等地的俯冲速度产生差异,俯冲板片局部发生撕裂,导致从内陆向沿海(粤东北-赣南-闽西南)逐渐裂开,形成裂隙或板片窗(图12).板片窗或裂隙为软流圈地幔物质上涌提供了空间,板片下部的软流圈地幔物质沿板片窗或裂隙上涌,将大洋板片上沉积物卷裹一起上升,软流圈上涌加剧了伸展构造运动的发展,为基性岩墙原生岩浆的形成提供了空间。

早一中侏罗世(190~170 Ma)的南岭东段处于拉张裂解构造体系,属板内伸展构造产物,发育典型的双峰式火山岩(Li *et al.*, 2003;章邦桐等,2004; Cen *et al.*, 2016)和基性岩墙(Zhang *et al.*, 2018)。

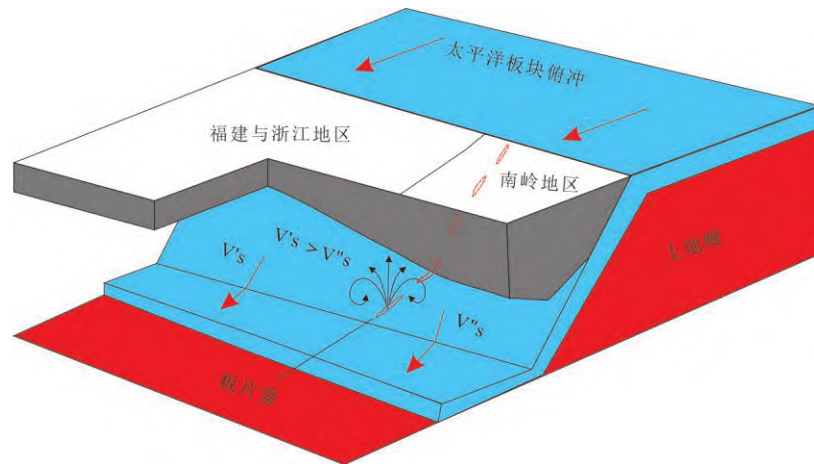


图 12 闽西南基性岩墙形成的大地构造演化模式

Fig.12 Geotectonic evolution model of mafic dyke formation in Southwest Fujian

中—晚侏罗世中国东南部几乎没有代表岩石圈伸展的岩石组合出现,标志着印支期造山后伸展裂解的结束,逐渐进入了太平洋构造域的活动大陆边缘挤压造山阶段,挤压为主体构造,但局部或某一阶段会出现短暂的岩石圈伸展构造现象(Wang *et al.*, 2013, 2016);南岭地区出露有地幔物质加入的过渡类型 S 花岗岩或 I 型花岗岩(Jia *et al.*, 2020; Liu *et al.*, 2020),表明中—晚侏罗世南岭地区处于挤压与伸展相互交替的背景下(Liu *et al.*, 2020)。中—晚侏罗世太平洋板块持续俯冲挤压,古太平洋构造域逐渐占据主导,南岭地区的大洋板片俯冲速率虽受到影响,因能量积累不足,板片上可能出现短暂的裂隙,软流圈地幔物质通过裂隙上涌所形成的玄武质岩浆无足够能量到达地表,只能到达地壳内致使地壳物质部分熔融,形成南岭过渡类型或非典型 S 花岗岩或 I 型花岗岩(Li *et al.*, 2007; Jia *et al.*, 2020; Liu *et al.*, 2020)。白垩纪以来,太平洋板块呈 NW 斜向大规模快速俯冲,因南岭地区褶皱带下部的巨厚岩石圈的阻挡,导致大洋板片的俯冲相对速率下降,板片受力不均,板片发生撕裂,形成裂隙或板片窗。软流圈地幔物质沿裂隙或板片窗上涌,并促使大洋沉积物发生低度熔融,与亏损地幔橄榄岩发生交代作用,形成富集地幔组分。随着软流圈地幔持续强烈上涌,富集地幔组分伴随着软流圈地幔上升至浅部发生部分熔融,形成具有 E-MORB 特征的玄武质岩浆(图 12)。随着古太平洋板块持续俯冲和板片的后撤,板片上的裂隙或板片窗沿着粤东北—赣南—闽西南向沿海方向发育,基性岩墙形成时代由西向东逐渐变新,如粤东北的 140 Ma 基性岩墙出

露(李献华等, 1997),到研究区闽西南形成 117.4 Ma 的基性岩墙。因此,晚中生代纵横南岭的褶皱带阻碍了太平洋板片的快速俯冲,导致与邻区在俯冲速率上产生差异,造成应力不一致,使下插到南岭地区的板片出现了大型裂隙或板片窗,导致 E-MORB 型富集地幔岩石的形成。由于软流圈地幔的持续上涌,加剧了岩石圈的伸展,约在 117 Ma 中国东南部发生一期伸展作用,具有 E-MORB 地球化学特征的玄武质岩浆沿拉张裂隙上侵形成了闽西南基性岩墙。

5 结论

通过对闽西南早白垩世基性岩墙的岩石学、锆石 U-Pb 年代学、元素地球化学和同位素地球化学研究,取得以下认识。

(1) 闽西南基性岩墙锆石 U-Pb 年龄为 117.4 ± 3.8 Ma,属于中国东南部早白垩世晚期大陆拉张—陆内初始裂谷阶段的岩浆活动产物。

(2) 闽西南基性岩墙为中—低钾岩石系列,具有弱富集稀土元素,富集 Rb、Ba、U 和 K 等大离子亲石元素,无 Nb、Ta 和 Ti 负异常的地球化学特征,岩浆演化过程中未受到明显的地壳混染作用影响。

(3) Sr-Nd 同位素和元素地球化学研究表明,闽西南基性岩墙地幔源区具有富集大洋中脊玄武岩(E-MORB)特征。结合中国东南部晚中生代大地构造演化的特征,推测由于近 EW 向巨厚南岭岩石圈的阻碍,导致古太平洋板块俯冲速率下降,造成板片下插速率与邻区发生差异,俯冲板片受力不均,板片局部发生撕裂现象,产生大型裂缝或板片

窗,软流圈地幔沿裂缝或板片窗减压上涌卷裹海洋沉积物上升发生部分熔融,形成了闽西南的基性岩墙原始岩浆。

致谢:野外工作得到了福建省地质调查研究院的陈润生总工程师、许美辉高级工程师大力支持和帮助;论文在写作过程中中国地质大学(武汉)吴元保教授、西北大学刘燊研究员给予了很好的建议;两位匿名审稿人提出的修改意见,对提升论文质量起到重要作用,作者谨此致以诚挚谢意!

附表见地球科学官网(<http://www.earth-science.net>)。

References

- Andersen, T., 2002. Correction of Common Lead in U-Pb Analyses That Do Not Report ^{204}Pb . *Chemical Geology*, 192(1–2): 59–79.
- Arevalo, R. Jr., McDonough, W. F., Luong, M., 2009. The K/U Ratio of the Silicate Earth: Insights into Mantle Composition, Structure and Thermal Evolution. *Earth and Planetary Science Letters*, 278(3–4): 361–369. <https://doi.org/10.1016/j.epsl.2008.12.023>
- Cabanis, B., Lecolle, M., 1989. Le Diagramme La/10-Y/15-N/8: Un Outil Pour La Discrimination Des Séries Volcaniques et La Mise en Évidence Des Processus De Mélange et/ou de Contamination Crustale. *Comptes Rendues de la Academie des Sciences Série IIA*, 309(20): 2023–2029.
- Cao, J. J., Hu, R. Z., Xie, G. Q., et al., 2009. Geochemistry and Genesis of Mafic Dikes from the Coastal Areas of Guangdong Province, China. *Acta Petrologica Sinica*, 25(4): 984–1000 (in Chinese with English abstract).
- Cen, T., Li, W. X., Wang, X. C., et al., 2016. Petrogenesis of Early Jurassic Basalts in Southern Jiangxi Province, South China: Implications for the Thermal State of the Mesozoic Mantle beneath South China. *Lithos*, 256–257: 311–330. <https://doi.org/10.1016/j.lithos.2016.03.022>
- Chen, X. Y., Wang, Y. J., Han, H. P., et al., 2014. Geochemical and Geochronological Characteristics of Triassic Basic Dikes in SW Hainan Island and Its Tectonic Implications. *Journal of Jilin University (Earth Science Edition)*, 44(3): 835–847 (in Chinese with English abstract).
- Cui, Y. Y., Zhao, Z. D., Jiang, T., et al., 2013. Geochronology, Geochemistry and Petrogenesis of the Early Paleozoic Granitoids in Southern Jiangxi Province, China. *Acta Petrologica Sinica*, 29(11): 4011–4024 (in Chinese with English abstract).
- Dilek, Y., 2006. Collision Tectonics of the Mediterranean Region: Causes and Consequences. *Geological Society of America Special Papers*, 409: 1–13. [https://doi.org/10.1130/2006.2409\(01\)](https://doi.org/10.1130/2006.2409(01))
- Ding, C., Zhao, Z. D., Yang, J. B., et al., 2015. Geochronology, Geochemistry of the Cretaceous Granitoids and Mafic to Intermediate Dykes in Shishi Area, Coastal Fujian Province. *Acta Petrologica Sinica*, 31(5): 1433–1447 (in Chinese with English abstract).
- Dong, C. W., Yan, Q., Zhang, D. R., et al., 2010. Late Mesozoic Extension in the Coastal Area of Zhejiang and Fujian Provinces: A Petrologic Indicator from the Dongji Island Mafic Dike Swarms. *Acta Petrologica Sinica*, 26(4): 1195–1203 (in Chinese with English abstract).
- Dong, C. W., Zhou, C., Gu, H. Y., et al., 2011. The Age Difference, Geochemistry and Petrogenesis of Mafic Dikes and Host Granites from Meizhou Island in Fujian Province. *Journal of Jilin University (Earth Science Edition)*, 41(3): 735–744 (in Chinese with English abstract).
- Donnelly, K. E., Goldstein, S. L., Langmuir, C. H., et al., 2004. Origin of Enriched Ocean Ridge Basalts and Implications for Mantle Dynamics. *Earth and Planetary Science Letters*, 226(3–4): 347–366. <https://doi.org/10.1016/j.epsl.2004.07.019>
- Ernst, R. E., 2014. Large Igneous Provinces. Cambridge University Press, Cambridge. <https://doi.org/10.1017/cbo9781139025300>
- Fitton, J. G., Saunders, A. D., Norry, M. J., et al., 1997. Thermal and Chemical Structure of the Iceland Plume. *Earth and Planetary Science Letters*, 153(3–4): 197–208. [https://doi.org/10.1016/s0012-821x\(97\)00170-2](https://doi.org/10.1016/s0012-821x(97)00170-2)
- Gilder, S. A., Gill, J., Coe, R. S., et al., 1996. Isotopic and Paleomagnetic Constraints on the Mesozoic Tectonic Evolution of South China. *Journal of Geophysical Research: Solid Earth*, 101(B7): 16137–16154. <https://doi.org/10.1029/96jb00662>
- Green, N. L., 2006. Influence of Slab Thermal Structure on Basalt Source Regions and Melting Conditions: REE and HFSE Constraints from the Garibaldi Volcanic Belt, Northern Cascadia Subduction System. *Lithos*, 87(1–2): 23–49. <https://doi.org/10.1016/j.lithos.2005.05.003>
- Hall, L. S., Mahoney, J. J., Sinton, J. M., et al., 2006. Spatial and Temporal Distribution of AC-Like Asthenospheric Component in the Rano Rahi Seamount Field, East Pacific Rise, 15°–19°S. *Geochemistry, Geophysics, Geosystems*, 7(3): Q03009. <https://doi.org/10.1029/2005gc000994>
- Hirschmann, M. M., Stolper, E. M., 1996. A Possible Role for Garnet Pyroxenite in the Origin of the “Garnet Signa-

- ture" in MORB. *Contributions to Mineralogy and Petrology*, 124(2): 185–208. <https://doi.org/10.1007/s004100050184>
- Ho, K.S., Chen, J.C., Lo, C.H., et al., 2003. ^{40}Ar - ^{39}Ar Dating and Geochemical Characteristics of Late Cenozoic Basaltic Rocks from the Zhejiang-Fujian Region, SE China: Eruption Ages, Magma Evolution and Petrogenesis. *Chemical Geology*, 197(1–4): 287–318. [https://doi.org/10.1016/s0009-2541\(02\)00399-6](https://doi.org/10.1016/s0009-2541(02)00399-6)
- Hofmann, A.W., 1988. Chemical Differentiation of the Earth: The Relationship between Mantle, Continental Crust, and Oceanic Crust. *Earth and Planetary Science Letters*, 90(3): 297–314. [https://doi.org/10.1016/0012-821x\(88\)90132-x](https://doi.org/10.1016/0012-821x(88)90132-x)
- Hou, G.T., Santosh, M., Qian, X.L., et al., 2008. Configuration of the Late Paleoproterozoic Supercontinent Columbia: Insights from Radiating Mafic Dyke Swarms. *Gondwana Research*, 14(3): 395–409. <https://doi.org/10.1016/j.gr.2008.01.010>
- Huang, Q.Z., Zhuang, J.M., Zheng, J.S., et al., 1998. Directions on Geological Map at Scale of 1:500 000 of Fujian Province. Fujian Map Publishing Press, Fuzhou, Attached Drawings, 1–4 (in Chinese).
- Jia, L.H., Mao, J.W., Liu, P., et al., 2020. Crust-Mantle Interaction during Subduction Zone Processes: Insight from Late Mesozoic I-Type Granites in Eastern Guangdong, SE China. *Journal of Asian Earth Sciences*, 192: 104284. <https://doi.org/10.1016/j.jseaes.2020.104284>
- John, B.M., Zhou, X.H., Li, J.L., 1990. Formation and Tectonic Evolution of Southeastern China and Taiwan: Isotopic and Geochemical Constraints. *Tectonophysics*, 183(1–4): 145–160. [https://doi.org/10.1016/0040-1951\(90\)90413-3](https://doi.org/10.1016/0040-1951(90)90413-3)
- Kong, X.G., 2001. Geochemistry Perogenesis of Early Yanshanian Volcanic and the Relationship of Uranium Deposit, South Jiangxi Province (Dissertation). Nanjing University, Nanjing, 7–18 (in Chinese with English abstract).
- Lapierre, H., Jahn, B.M., Charvet, J., et al., 1997. Mesozoic Felsic Arc Magmatism and Continental Olivine Tholeiites in Zhejiang Province and Their Relationship with the Tectonic Activity in Southeastern China. *Tectonophysics*, 274(4): 321–338. [https://doi.org/10.1016/s0040-1951\(97\)00009-7](https://doi.org/10.1016/s0040-1951(97)00009-7)
- Lei, Z.L., Zeng, G., Wang, X.J., et al., 2019. Mantle Source Lithology of Late Mesozoic Mafic Dikes in Southeastern China. *Earth Science*, 44(4): 1159–1168 (in Chinese with English abstract).
- Li, X.H., Chen, Z.G., Liu, D.Y., et al., 2003. Jurassic Gabbro-Granite-Syenite Suites from Southern Jiangxi Province, SE China: Age, Origin, and Tectonic Significance. *International Geology Review*, 45(10): 898–921. <https://doi.org/10.2747/0020-6814.45.10.898>
- Li, X.H., Hu, R.Z., Rao, B., 1997. Geochronology and Geochemistry of Cretaceous Mafic Dikes from Northern Guangdong, SE China. *Geochimica*, 26(2): 14–31 (in Chinese with English abstract).
- Li, X.H., Li, Z.X., Li, W.X., et al., 2007. U-Pb Zircon, Geochemical and Sr-Nd-Hf Isotopic Constraints on Age and Origin of Jurassic I- and A-Type Granites from Central Guangdong, SE China: A Major Igneous Event in Response to Foundering of a Subducted Flat-Slab? *Lithos*, 96(1–2): 186–204. <https://doi.org/10.1016/j.lithos.2006.09.018>
- Li, Y.Q., Ma, C.Q., Robinson, P.T., et al., 2015. Recycling of Oceanic Crust from a Stagnant Slab in the Mantle Transition Zone: Evidence from Cenozoic Continental Basalts in Zhejiang Province, SE China. *Lithos*, 230: 146–165. <https://doi.org/10.1016/j.lithos.2015.05.021>
- Li, Z.X., Li, X.H., 2007. Formation of the 1 300 km Wide Intracontinental Orogen and Postorogenic Magmatic Province in Mesozoic South China: A Flat-Slab Subduction Model. *Geology*, 35(2): 179–182. <https://doi.org/10.1130/g23193a.1>
- Liang, X.R., Wei, G.J., Li, X.H., et al., 2003. Precise Measurement of $^{143}\text{Nd}/^{144}\text{Nd}$ and Sm/Nd Ratios Using Multiple Collectors-Inductively Coupled Plasma Mass Spectrometer (MC-ICPMS). *Geochimica*, 32(1): 92–97 (in Chinese with English abstract).
- Liu, L., Xu, X.S., Xia, Y., 2016. Asynchronizing Paleo-Pacific Slab Rollback beneath SE China: Insights from the Episodic Late Mesozoic Volcanism. *Gondwana Research*, 37: 397–407. <https://doi.org/10.1016/j.gr.2015.09.009>
- Liu, X., Wang, Q., Ma, L., et al., 2020. Petrogenesis of Late Jurassic Two-Mica Granites and Associated Diorites and Syenite Porphyries in Guangzhou, SE China. *Lithos*, 364–365: 105537. <https://doi.org/10.1016/j.lithos.2020.105537>
- Maurice, A.E., Basta, F.F., Khiamy, A.A., 2012. Neoproterozoic Nascent Island Arc Volcanism from the Nubian Shield of Egypt: Magma Genesis and Generation of Continental Crust in Intra-Oceanic Arcs. *Lithos*, 132–133: 1–20. <https://doi.org/10.1016/j.lithos.2011.11.013>
- Meng, L.F., Li, Z.X., Chen, H.L., et al., 2012. Geochronological and Geochemical Results from Mesozoic Basalts in Southern South China Block Support the Flat-Slab Sub-

- duction Model. *Lithos*, 132–133: 127–140. <https://doi.org/10.1016/j.lithos.2011.11.022>
- Middlemost, E. A. K., 1994. Naming Materials in the Magma/Igneous Rock System. *Earth-Science Reviews*, 37(3–4): 215–224. [https://doi.org/10.1016/0012-8252\(94\)90029-9](https://doi.org/10.1016/0012-8252(94)90029-9)
- Niu, Y. L., Regelous, M., Wendt, I. J., et al., 2002. Geochemistry of Near-EPR Seamounts: Importance of Source vs. Process and the Origin of Enriched Mantle Component. *Earth and Planetary Science Letters*, 199(3–4): 327–345. [https://doi.org/10.1016/s0012-821x\(02\)00591-5](https://doi.org/10.1016/s0012-821x(02)00591-5)
- Pearce, J. A., 2008. Geochemical Fingerprinting of Oceanic Basalts with Applications to Ophiolite Classification and the Search for Archean Oceanic Crust. *Lithos*, 100(1–4): 14–48. <https://doi.org/10.1016/j.lithos.2007.06.016>
- Peng, P., 2015. Precambrian Mafic Dyke Swarms in the North China Craton and Their Geological Implications. *Science China Earth Sciences*, 58(5): 649–675. <https://doi.org/10.1007/s11430-014-5026-x>
- Plank, T., Ludden, J. N., 1992. Geochemistry of Sediments in the Argo Abyssal Plain at Site 765: A Continental Margin Reference Section for Sediment Recycling in Subduction Zones. In: Gradstein, F. M., Ludden, J. N., et al., eds., Proc. ODP, Sci. Results, 123: College Station, TX (Ocean Drilling Program), 167–189. <https://doi.org/10.2973/odp.proc.sr.123.158.1992>
- Qi, L., Hu, J., Gregoire, D. C., 2000. Determination of Trace Elements in Granites by Inductively Coupled Plasma Mass Spectrometry. *Talanta*, 51: 507–513. [https://doi.org/10.1016/s0039-9140\(99\)00318-5](https://doi.org/10.1016/s0039-9140(99)00318-5)
- Qin, S. C., Fan, W. M., Guo, F., et al., 2010. Petrogenesis of Late Mesozoic Diabase Dikes in Zhejiang-Fujian Provinces: Constraints from Ar-Ar Dating and Geochemistry. *Acta Petrologica Sinica*, 26(11): 3295–3306 (in Chinese with English abstract).
- Rickwood, P. C., 1989. Boundary Lines within Petrologic Diagrams Which Use Oxides of Major and Minor Elements. *Lithos*, 22(4): 247–263. [https://doi.org/10.1016/0024-4937\(89\)90028-5](https://doi.org/10.1016/0024-4937(89)90028-5)
- Shimizu, K., Saal, A. E., Myers, C. E., et al., 2016. Two-Component Mantle Melting-Mixing Model for the Generation of Mid-Ocean Ridge Basalts: Implications for the Volatile Content of the Pacific Upper Mantle. *Geochimica et Cosmochimica Acta*, 176: 44–80. <https://doi.org/10.1016/j.gca.2015.10.033>
- Shu, L. S., Zhou, X. M., Deng, P., et al., 2009. Mesozoic Tectonic Evolution of the Southeast China Block: New Insights from Basin Analysis. *Journal of Asian Earth Sciences*, 34(3): 376–391. <https://doi.org/10.1016/j.jseas.2008.06.004>
- Smith, M. C., Perfit, M. R., Fornari, D. J., et al., 2001. Magmatic Processes and Segmentation at a Fast Spreading Mid-Ocean Ridge: Detailed Investigation of an Axial Discontinuity on the East Pacific Rise Crest at 9°37'N. *Geochemistry, Geophysics, Geosystems*, 2(10): 2000GC000134. <https://doi.org/10.1029/2000gc000134>
- Song, M. J., Shu, L. S., Santosh, M., 2017. Early Mesozoic Intracontinental Orogeny and Stress Transmission in South China: Evidence from Triassic Peraluminous Granites. *Journal of the Geological Society*, 174(3): 591–607. <https://doi.org/10.1144/jgs2016-098>
- Srivastava, R. K., Söderlund, U., Ernst, R. E., et al., 2019. Precambrian Mafic Dyke Swarms in the Singhbhum Craton (Eastern India) and Their Links with Dyke Swarms of the Eastern Dharwar Craton (Southern India). *Precambrian Research*, 329: 5–17. <https://doi.org/10.1016/j.precamres.2018.08.001>
- Sun, S. Q., Wang, Y. L., Zhang, C. J., 2003. Discrimination of the Tectonic Settings of Basalts by Th, Nb and Zr. *Geological Review*, 49(1): 40–47 (in Chinese with English abstract).
- Sun, S. S., McDonough, W. F., 1989. Chemical and Isotopic Systematics of Oceanic Basalts: Implications for Mantle Composition and Processes. *Geological Society, London, Special Publications*, 42(1): 313–345. <https://doi.org/10.1144/gsl.sp.1989.042.01.19>
- Sun, T., Zhou, X. M., Chen, P. R., et al., 2005. Strongly Peraluminous Granites of Mesozoic in Eastern Nanling Range, Southern China: Petrogenesis and Implications for Tectonics. *Science in China Earth Sciences*, 48(2): 165–174. <https://doi.org/10.1360/03yd0042>
- Tang, L. M., Chen, H. L., Dong, C. W., et al., 2010. Late Mesozoic Tectonic Extension in SE China: Evidence from the Basic Dike Swarms in Hainan Island, China. *Acta Petrologica Sinica*, 26(4): 1204–1216 (in Chinese with English abstract).
- Wang, G. C., Jiang, Y. H., Liu, Z., et al., 2016. Multiple Origins for the Middle Jurassic to Early Cretaceous High-K Calc-Alkaline I-Type Granites in Northwestern Fujian Province, SE China and Tectonic Implications. *Lithos*, 246–247: 197–211. <https://doi.org/10.1016/j.lithos.2015.12.022>
- Wang, L. X., Ma, C. Q., Zhang, C., et al., 2018. Halogen Geochemistry of I- and A-Type Granites from Jiuhuashan Region (South China): Insights into the Elevated Fluorine in A-Type Granite. *Chemical Geology*, 478: 164–182.

- <https://doi.org/10.1016/j.chemgeo.2017.09.033>
- Wang, Y. J., Fan, W. M., Peng, T. P., et al., 2005. Elemental and Sr-Nd Isotopic Systematics of the Early Mesozoic Volcanic Sequence in Southern Jiangxi Province, South China: Petrogenesis and Tectonic Implications. *International Journal of Earth Sciences*, 94(1): 53–65. <https://doi.org/10.1007/s00531-004-0441-4>
- Wang, Y. J., Fan, W. M., Zhang, G. W., et al., 2013. Phanerozoic Tectonics of the South China Block: Key Observations and Controversies. *Gondwana Research*, 23(4): 1273–1305.
- Wedepohl, K. H., 1995. The Composition of the Continental Crust. *Geochimica et Cosmochimica Acta*, 59(7): 1217–1232. [https://doi.org/10.1016/0016-7037\(95\)00038-2](https://doi.org/10.1016/0016-7037(95)00038-2)
- Wood, D. A., 1980. The Application of a Th-Hf-Ta Diagram to Problems of Tectonomagmatic Classification and to Establishing the Nature of Crustal Contamination of Basaltic Lavas of the British Tertiary Volcanic Province. *Earth and Planetary Science Letters*, 50(1): 11–30. [https://doi.org/10.1016/0012-821x\(80\)90116-8](https://doi.org/10.1016/0012-821x(80)90116-8)
- Xie, G. Q., Hu, R. Z., Mao, J. W., et al., 2006. K-Ar Dating, Geochemical, and Sr-Nd-Pb Isotopic Systematics of Late Mesozoic Mafic Dikes, Southern Jiangxi Province, Southeast China: Petrogenesis and Tectonic Implications. *International Geology Review*, 48(11): 1023–1051. <https://doi.org/10.2747/0020-6814.48.11.1023>
- Xu, X. B., Zhang, Y. Q., Jia, D., et al., 2009. Early Mesozoic Geotectonic Processes in South China. *Geology in China*, 36(3): 573–593 (in Chinese with English abstract).
- Yang, J. B., 2015. Petrological and Geochemical Studies of the Cenozoic Basalts and Hosted Peridotite Xenoliths in Zhejiang and Fujian Provinces (Dissertation). China University of Geosciences, Beijing (in Chinese with English abstract).
- Yang, J. B., Zhao, Z. D., Hou, Q. Y., et al., 2018. Petrogenesis of Cretaceous (133–84 Ma) Intermediate Dykes and Host Granites in Southeastern China: Implications for Lithospheric Extension, Continental Crustal Growth, and Geodynamics of Palaeo-Pacific Subduction. *Lithos*, 296–299: 195–211. <https://doi.org/10.1016/j.lithos.2017.10.022>
- Yuan, H. L., Gao, S., Dai, M. N., et al., 2008. Simultaneous Determinations of U-Pb Age, Hf Isotopes and Trace Element Compositions of Zircon by Excimer Laser-Ablation Quadrupole and Multiple-Collector ICP-MS. *Chemical Geology*, 247(1–2): 100–118. <https://doi.org/10.1016/j.chemgeo.2007.10.003>
- Zhang, B., Guo, F., Zhang, X. B., et al., 2019. Early Cretaceous Subduction of Paleo-Pacific Ocean in the Coastal Region of SE China: Petrological and Geochemical Constraints from the Mafic Intrusions. *Lithos*, 334–335: 8–24. <https://doi.org/10.1016/j.lithos.2019.03.010>
- Zhang, B. T., Chen, P. R., Ling, H. F., et al., 2004. Geochemistry and Petrogenesis of the Middle Jurassic Rhyolite, Southern Jiangxi: Trace Element and Pb-Nd-Sr Isotope Geochemical Constraints on the Upper Crustal Origin. *Acta Petrologica Sinica*, 20(3): 511–520 (in Chinese with English abstract).
- Zhang, D., Zhao, K. D., Chen, W., et al., 2018. Early Jurassic Mafic Dykes from the Aigao Uranium Ore Deposit in South China: Geochronology, Petrogenesis and Relationship with Uranium Mineralization. *Lithos*, 308–309: 118–133. <https://doi.org/10.1016/j.lithos.2018.02.028>
- Zhang, G. S., Liu, S. W., Han, W. H., et al., 2017. Baddeleyite U-Pb Age and Geochemical Data of the Mafic Dykes from South Qinling: Constraints on the Lithospheric Extension. *Geological Journal*, 52: 272–285. <https://doi.org/10.1002/gj.3074>
- Zhang, G. S., Wen, H. J., Hu, R. Z., et al., 2007. Genesis and Dynamic Setting of Mafic Dikes in Southeastern Fujian: Evidence from Sr-Nd Isotopic and Major and Trace Element Geochemistry. *Acta Petrologica Sinica*, 23(4): 793–804 (in Chinese with English abstract).
- Zhang, G. S., Wen, H. J., Hu, R. Z., et al., 2007. Geochemistry of Late Mesozoic Mafic Dykes in Western Fujian Province of China: Sr-Nd Isotope and Trace Element Constraints. *Chinese Journal of Geochemistry*, 26(2): 143–156. <https://doi.org/10.1007/s11631-007-0143-2>
- Zhang, J. H., Wang, H. C., Guo, J. H., et al., 2020. Metamorphic Mafic Dykes from Tianzhen-Huai'an Area: Transformation Criteria of the Late Paleoproterozoic. *Earth Sciences*, 45(9): 3239–3257 (in Chinese with English abstract).
- Zhao, J. H., Hu, R. Z., Liu, S., 2004. Geochemistry, Petrogenesis, and Tectonic Significance of Mesozoic Mafic Dikes, Fujian Province, Southeastern China. *International Geology Review*, 46(6): 542–557. <https://doi.org/10.2747/0020-6814.46.6.542>
- Zhao, J. H., Hu, R. Z., Zhou, M. F., et al., 2007. Elemental and Sr-Nd-Pb Isotopic Geochemistry of Mesozoic Mafic Intrusions in Southern Fujian Province, SE China: Implications for Lithospheric Mantle Evolution. *Geological Magazine*, 144(6): 937–952.
- Zhou, X. M., Sun, T., Shen, W. Z., et al., 2006. Petrogenesis of Mesozoic Granitoids and Volcanic Rocks in South China: A Response to Tectonic Evolution. *Episodes*, 29(1): 26–

33.<https://doi.org/10.18814/epiiugs/2006/v29i1/004>

- Zindler, A., Hart, S., 1986. Chemical Geodynamics. *Annual Review of Earth and Planetary Sciences*, 14(1): 493–571. <https://doi.org/10.1146/annurev.ea.14.050186.002425>
- Zou, H.B., Zindler, A., Xu, X.S., et al., 2000. Major, Trace Element, and Nd, Sr and Pb Isotope Studies of Cenozoic Basalts in SE China: Mantle Sources, Regional Variations, and Tectonic Significance. *Chemical Geology*, 171(1–2): 33–47. [https://doi.org/10.1016/s0009-2541\(00\)00243-6](https://doi.org/10.1016/s0009-2541(00)00243-6)

附中文参考文献

- 曹建劲, 胡瑞忠, 谢桂青, 等, 2009. 广东沿海地区基性岩脉地球化学及成因. *岩石学报*, 25(4): 984–1000.
- 陈新跃, 王岳军, 韩会平, 等, 2014. 琼西南三叠纪基性岩脉年代学、地球化学特征及其构造意义. *吉林大学学报(地球科学版)*, 44(3): 835–847.
- 崔圆圆, 赵志丹, 蒋婷, 等, 2013. 赣南早古生代晚期花岗岩类年代学、地球化学及岩石成因. *岩石学报*, 29(11): 4011–4024.
- 丁聪, 赵志丹, 杨金豹, 等, 2015. 福建石狮白垩纪花岗岩与中基性脉岩的年代学与地球化学. *岩石学报*, 31(5): 1433–1447.
- 董传万, 闫强, 张登荣, 等, 2010. 浙闽沿海晚中生代伸展构造的岩石学标志: 东极岛镁铁质岩墙群. *岩石学报*, 26(4): 1195–1203.
- 董传万, 周超, 顾虹艳, 等, 2011. 福建湄州岛镁铁质岩墙群与寄主花岗岩的形成时差、地球化学及成因. *吉林大学学报(地球科学)*, 41(3): 735–744.
- 黄泉祯, 庄建民, 郑声俭, 等, 1998. 福建省地质图(1:500 000)说明书. 福州: 福建省地图出版社, 附图, 1–4.
- 孔兴功, 2001. 赣南燕山早期火山岩地球化学成因及与铀成矿关系(博士学位论文). 南京: 南京大学, 7–18.
- 雷祝梁, 曾罡, 王小均, 等, 2019. 中国东南部晚中生代基性岩脉地幔源区的岩性演化历史. *地球科学*, 44(4): 1159–1170.
- 李献华, 胡瑞忠, 饶冰, 1997. 粤北白垩纪基性岩脉的年代学和地球化学. *地球化学*, 26(2): 14–31.
- 梁细荣, 韦刚健, 李献华, 等, 2003. 利用 MC-ICPMS 精确测定 $^{143}\text{Nd}/^{144}\text{Nd}$ 和 Sm/Nd 比值. *地球化学*, 32(1): 92–97.
- 秦社彩, 范蔚茗, 郭锋, 等, 2010. 浙闽晚中生代辉绿岩脉的岩石成因: 年代学与地球化学制约. *岩石学报*, 26(11): 3295–3306.
- 孙书勤, 汪云亮, 张成江, 2003. 玄武岩类岩石大地构造环境的 Th、Nb、Zr 判别. *地质论评*, 49(1): 40–47.
- 唐立梅, 陈汉林, 董传万, 等, 2010. 中国东南部晚中生代构造伸展作用: 来自海南岛基性岩墙群的证据. *岩石学报*, 26(4): 1204–1216.
- 徐先兵, 张岳桥, 贾东, 等, 2009. 华南早中生代大地构造过程. *中国地质*, 36(3): 573–593.
- 杨金豹, 2015. 浙闽地区新生代玄武岩和地幔捕虏体岩石学与地球化学(博士学位论文). 北京: 中国地质大学.
- 章邦桐, 陈培荣, 凌洪飞, 等, 2004. 赣南中侏罗世流纹岩地球化学及成因研究: 上地壳成因的微量元素和 Pb-Nd-Sr 同位素地球化学制约. *岩石学报*, 20(3): 511–520.
- 张贵山, 温汉捷, 胡瑞忠, 等, 2007. 闽东南基性岩脉成因及动力学背景研究: Sr-Nd 同位素、元素地球化学. *岩石学报*, 23(4): 793–804.
- 张家辉, 王惠初, 郭敬辉, 等, 2020. 天镇—怀安地区变质基性岩墙群: 华北克拉通古元古代末期碰撞—伸展构造体制转换标志. *地球科学*, 45(9): 3239–3257.